A. Sugerman

S. Schmidt

Y. O. Tu

# Strain and Temperature Distributions in a Thermally Activated Cantilever

This communication describes the use of a mathematical model to predict the behavior of an electromechanical semiconductor oscillator. The device being simulated is a silicon cantilever (Fig. 1), free at one end, periodically heated on a small segment of one surface by an embedded resistor, and having as heat sink the fixed-end mechanical support (pedestal) on the opposite surface. The model defines the strain and temperature distributions in the cantilever as functions of geometry, material constants, and input power; its application is to determine the conditions that will maximize strain in the region near the pedestal for a specified power source. Although experimental results are given only for the device described, the model is analytically general enough to permit the manipulation of parameters for design purposes.

The equation of motion is based on a thermodynamic potential that is consistent with our expectations for the solution; that is, we have assumed that the potential includes only such terms as will reproduce the properties of interest in the cantilever. All other interactions are considered to be higher-order effects and external forces are ignored. (We assume, for example, that the cantilever material is isotropic; if a more complex phenomenon were to be considered, the equation of motion would reflect the addition of appropriate terms to the potential.) By applying Hamilton's principle to a generalized potential and including an energy dissipation term to account for damping, the equation of motion and the appropriate spatial boundary conditions can be rigorously developed.<sup>2,3</sup>

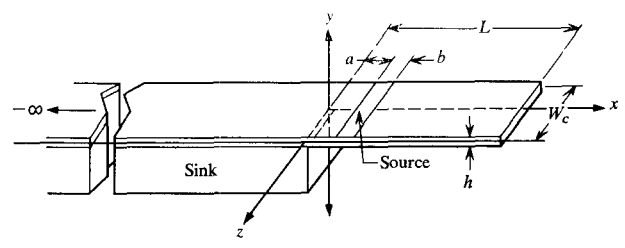


Figure 1 Cantilever geometry. (Approximate dimensions: L = 350 mils, h = 5 mils,  $W_c = 30$  mils, b = 5 mils.)

Under the simplifying assumptions, however, the equation for this model reduces to one obtainable from the Euler-Bernoulli simple beam theory.<sup>4,5</sup>

An analytical temperature distribution, found by the method of images, is used for heating frequencies above 10 Hz, leaving only cases approaching dc to be evaluated numerically. (A single numerical differentiation of a discrete-point field will yield reasonable accuracy for the low-frequency case.) The solution for strain distribution is given in integral form, which has only a first order derivative of the temperature distribution, so that solutions can be found for either type of temperature profile.

### **Equation of motion**

The equation of motion can be shown to be

$$(Eh^{3}/12)\partial_{x}^{4}w(x, t) + \rho h\partial_{t}^{2}w(x, t) - (\rho h^{3}/12)\partial_{x}^{2}\partial_{t}^{2}w(x, t) + c\partial_{t}w(x, t) = (\alpha E/3) \int_{-h/2}^{h/2} y \partial_{x}^{2}T(x, y, t) dy, \quad (1)$$

A. Sugerman and S. Schmidt are located at the IBM Components Division Laboratory, Poughkeepsie, New York; Y. O. Tu is located at the IBM Thomas J. Watson Research Center, Yorktown Heights, New York.

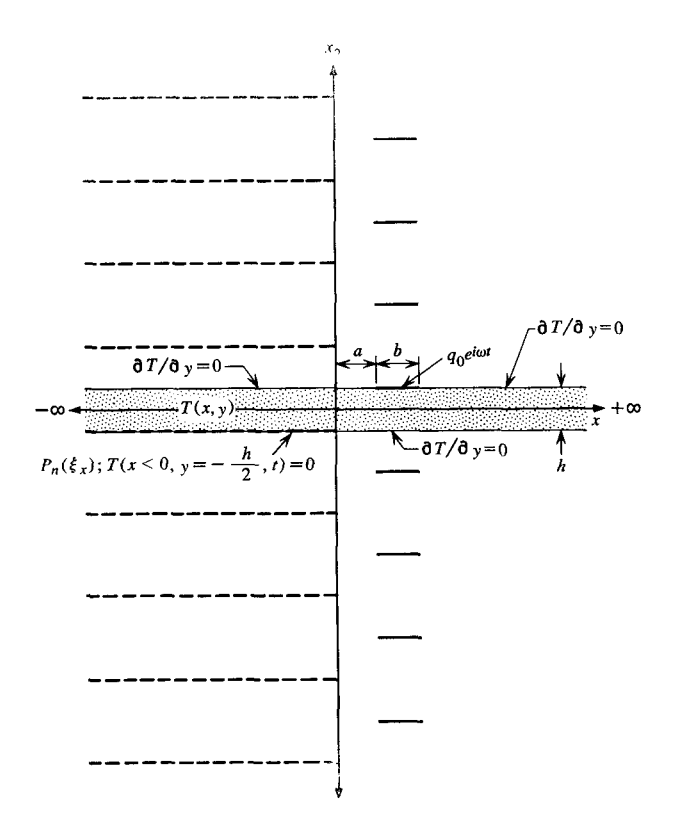


Figure 2 Method of images. The sink images (dashed lines) extend to  $-\infty$  in the x direction and there is an infinite number of sink and source (solid-line) images; a few are shown for illustration.

where w(x, t) is the displacement from the x axis of a point on the neutral axis of the cantilever; x, y, z and t are the Cartesian coordinates (Fig. 1) of the system and the time, respectively;  $\partial_x$  and  $\partial_t$  are partial differential operators with respect to x and t, respectively; E is Young's elastic modulus; h is the cantilever thickness;  $\rho$  is the cantilever material density; c is the coefficient of damping;  $\alpha$  is the coefficient of thermal expansion; and T is the temperature distribution.

Equation (1) is essentially that of a simple damped harmonic oscillator, with higher-order effects omitted under the assumptions given above (isotropic material, no external forces) and the approximation<sup>3</sup> that plane sections normal to the neutral axis at equilibrium remain so under thermal excitation. The damping is proportional to velocity and the coefficient c is determined empirically by measuring the time  $\tilde{t}$  required for the displacement amplitude to decay to 1/e of its resonant value. For the simple damped oscillator  $\tilde{t} = 2m/c$ , where m is the mass; for the cantilever we write  $t = 2\rho h/c$  for a point on the neutral axis. The quality Q of the device is also related to t by  $Q = \omega t/2$ , where  $\omega$  is the resonant frequency.

# Temperature distribution

The instantaneous power supplied to the heating element comprises a dc potential  $V_B$  and an ac potential  $V_G(\omega)$  applied across the element, and is given by

$$P = \frac{1}{R} (V_B + V_G \cos \omega t)^2 = \text{Re} \sum_{n=0}^{2} a_n \exp(in\omega t), \quad (2)$$

where R is the resistance of the heater and the  $a_n$  are  $(2V_B^2 + V_G^2)/2R$ ,  $2V_BV_G/R$ , and  $V_G^2/2R$  respectively.

The temperature distribution is a scalar quantity and can be written as a sum of terms corresponding to the Fourier components of the input power. The diffusion equation is

$$k(\partial_x^2 + \partial_y^2)T = \partial_t T, \tag{3}$$

where k is the coefficient of thermal diffusivity and  $\partial_v$  follows our convention. The point-source solution of Eq. (3) is integrated over the spatial extension of the periodic sources and sinks and over their temporal contributions. By applying steady-state conditions (i.e., heat sources turned on and heat sinks attached in the infinite past), a spatial boundary at infinity for the pedestal, and heater dimensions from x = a to x = a + b (Fig. 1), and by adding the contribution of each frequency component of the temperature, we have for the steady-state solution

$$T(x, y, t)$$

$$= \sum_{n=0}^{2} \left( \int_{-\infty}^{t} \frac{d\tau}{4\pi k(t-\tau)} \right)$$

$$\times \left\{ \int_{a}^{a+b} d\xi_{x} q_{0} \exp \left[ in\omega\tau - \frac{r^{2}}{4k(t-\tau)} \right] + \int_{-\infty}^{0} d\xi_{x} P_{n}(\xi_{x}) \exp \left[ in\omega\tau - \frac{r^{2}}{4k(t-\tau)} \right] \right\} \right), \quad (4)$$

where  $q_0$  is a constant proportional to the amplitude of the heat supply;

$$r = [(x - \xi_x)^2 + (y - \xi_y)^2]^{\frac{1}{2}};$$

 $\xi_x$  and  $\xi_y$  are source or sink coordinates parallel to x and y respectively; and  $P_n(\xi_x)$  is proportional to the amplitude of the heat absorption at the sink.

The assumptions made are that the pedestal is a perfect heat sink, i.e., that

$$T(x < 0, y = -h/2, t) = 0;$$
 (5)

that no heat is lost by convection at the surface; and that the temperature is not a function of z. (This last assumption is warranted because the cantilever is symmetric with respect to the x-y plane and is relatively wide, so that fringe effects can be ignored.) The temperature distribution is found by applying the method of images<sup>6</sup> (Fig. 2) to an infinite-strip approximation of the finite cantilever device. If the actual temperature approaches zero rapidly

enough at the ends of the cantilever, this an excellent assumption for the end conditions and the cantilever length  $\boldsymbol{L}$  can be assumed to be infinite. The steady-state temperature distribution satisfying the derivative boundary conditions is then

$$T(x, y, t) = \sum_{n=0}^{2} \varphi_{n}(x, y) \exp(in\omega t)$$

$$= \sum_{N=-\infty}^{\infty} \sum_{n=0}^{2} \frac{\exp(in\omega t)}{2\pi k} \left\{ \int_{a}^{a+b} d\xi_{x} q_{0} K_{0} \left[ \left( \frac{in\omega}{k} \right)^{\frac{1}{2}} \right] \right\}$$

$$\times \left\{ (x - \xi_{x})^{2} + \left[ y - \frac{(4N+1)h}{2} \right]^{2} \right\}^{\frac{1}{2}}$$

$$+ \int_{-\infty}^{0} d\xi_{x} P_{n}(\xi_{x}) K_{0} \left[ \left( \frac{in\omega}{k} \right)^{\frac{1}{2}} \right]$$

$$\times \left\{ (x - \xi_{x})^{2} + \left[ y - \frac{(4N-1)h}{2} \right]^{2} \right\}^{\frac{1}{2}} \right\}, \quad (6)$$

where  $K_0$  is the zero-order modified Bessel function of the second kind. This equation does not hold for frequencies approaching zero because the temperature at x = L does not approach zero for dc and because  $\partial_x T$  for x = L need not be zero in our model.

The unknown sink strength  $P_n(\xi_x)$  in Eq. (6) is determined uniquely by the boundary condition of Eq. (5) for each n, due to the independence of the sources. The  $P_n$ can be determined numerically by approximating the integrals by a two-point quadrature (trapezoidal rule) and collecting like terms of  $P_n$  at discrete points of  $\xi_x$  to obtain a complex linear system of equations in the complex variable unknown  $P_n$ . This system can be solved numerically using an existing Gauss-Jordan elimination subroutine with full pivoting.<sup>7</sup> The first integral term of Eq. (6) represents the constant terms of the linear system of equations and can be calculated directly; since its range of integration is the small distance b, fewer points are needed to span the range than are required for the second integral. It was found empirically that seventeen points are usually adequate. Since  $P_n$  is significant only near the source, an optimal step size for the second integral is 0.1h, or 0.5 mil for a nominal h of 5 mils. When the heating source is located in the positive half-plane, an adequate decay length for  $P_n$  is 24 intervals (12 mils), resulting in a 25  $\times$  25 matrix system. If the heater is located in the negative half-plane, however, a decay length of 48 intervals is needed and the matrix is  $49 \times 49$ .

The solution of Eq. (6) is approximated by numerical integration, except at the zeros of the  $K_0$  argument. In the region for which the argument  $i^{\frac{1}{2}}\gamma$  of  $K_0$  approaches zero, the asymptotic behavior of  $K_0$  is

$$\lim_{\gamma \to 0} K_0(i^{\frac{1}{2}}\gamma) = \lim_{\gamma \to 0} \ln \gamma + \text{constant}.$$

This function can be integrated analytically in the region  $0 + \leq \gamma \ll 1$  such that contributions by any smaller P are insignificant. For the numerical integration we use the alternative definition

$$K_0(i^{\frac{1}{2}}\gamma) = \ker(\gamma) + i \ker(\gamma),$$

where ker and kei are called Kelvin functions<sup>8</sup> and can be obtained easily by polynomial approximation within an error of  $10^{-8}$ .

The number N of images needed must be increased at very low frequencies. If we arbitrarily decide to ignore any contribution of the Bessel function  $K_0$  whose amplitude is less than  $e^{-2}$ , then the relation between N, the number of images necessary, and  $n\omega$  for acceptable N is

$$(2n\omega/k)^{\frac{1}{2}}Nh + (1/2) \ln \left[ (n\omega/k)^{\frac{1}{2}}Nh \right] = 4,$$
 (7)

as can be derived from the large-argument expansion of  $K_0$ .

#### Strain distribution

After separating temperature into sums of time- and spacedependent products, we can write the displacement response to the temperature driving force in a similar way:

$$w(x, t) = \sum_{n=0}^{2} \overline{w}_{n}(x) \exp(in\omega t), \qquad (8)$$

where  $\overline{w}_n(x)$  is defined by this equation and satisfies, for each n, the same boundary conditions as w(x, t), namely,

$$w(0, t) = \partial_x w(0, t) = 0;$$

$$\partial_x^2 w(L, t) + (4\alpha/h^3) \int_{-h/2}^{h/2} y T(y, L, t) dy = 0,$$

$$\partial_x^3 w(L, t) + (4\alpha/h^3) \int_{-h/2}^{h/2} y \partial_x T(y, L, t) dy = 0.$$
 (9b)

Equation (9a) corresponds to fixed conditions at x = 0, and Eqs. (9b) correspond to the presence of no moments or shearing forces at the free end, x = L. Using these conditions and dropping the third term in Eq. (1) as a useful corollary approximation, we have for the displacement

$$w(x, t) = (-4\alpha/h^3) \sum_{n=0}^{2} \exp(in\omega t) \int_{0}^{L} G_n(x, x')$$

$$\times \int_{-h/2}^{h/2} y' \partial_{x'}^{2} \varphi_n(x', y') dy' dx', \qquad (10)$$

where  $G_n(x, x')$  is the Green's function corresponding to the *n*'th component of displacement. (The Green's functions are linear combinations of trigonometric and hyperbolic functions, have continuous derivatives up to the third order at points in the cantilever, and satisfy the same boundary conditions as w.)

The strain distribution is obtained in a straightforward manner from Eq. (10), and is the real part of

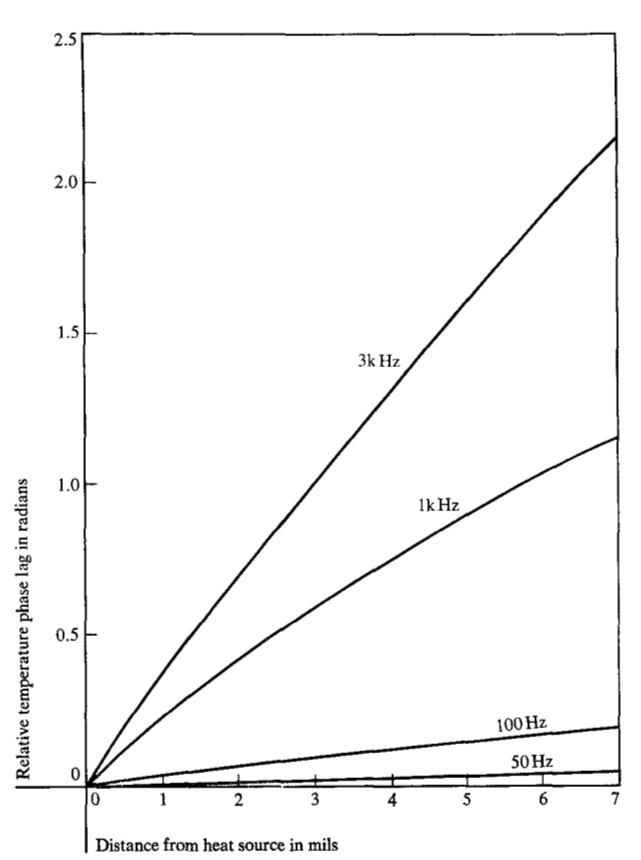
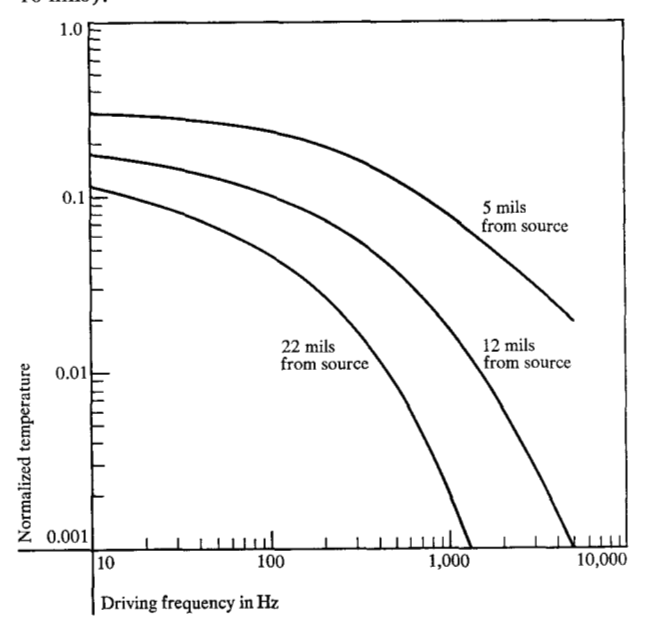


Figure 3 Phase lag of temperature at the upper surface relative to a point heat source located at x=-13 mils, vs. distance from the heat source.

Figure 4 Normalized temperature  $|\varphi(x)|/|\varphi_{\text{source}}$ ,  $\omega=10\,\text{Hz}|$  at the upper surface vs. heating frequency for various distances from a point source located at x=-13 miles (h=16 mils).



$$-y\partial_x^2 w(x, t) = (-4\alpha/h^3)y \sum_{n=0}^2 \exp(in\omega t)$$

$$\times \left[ \int_0^L \partial x' \, \partial_x^2 G_n(x, x') \right]$$

$$\times \int_{-h/2}^{h/2} y' \, \partial_{x'} \varphi_n(x', y') \, dy' \, dx' - \partial_x^2 G_n(x, 0)$$

$$\times \int_{-h/2}^{h/2} y' \, \partial_{x'} \varphi_n(0, y') \, dy' \right]. \tag{11}$$

## Results and discussion

Because a dc temperature distribution contributes negligibly to the strain and because the contribution of the  $2\omega$  mode to the temperature field and hence the strain can be made very small relative to the contribution of the  $\omega$  mode, the following discussion and the results presented are with respect to the  $\omega$  mode only. (The qualitative discussion is not affected by this restriction.)

At any instant, a temperature wave is propagated from the heating element at phase velocity

$$n\omega \left[\frac{d}{dx} \tan^{-1} \left(\frac{\operatorname{Im} \varphi_n}{\operatorname{Re} \varphi_n}\right)\right]^{-1} \cong (2kn\omega)^{\frac{1}{2}}$$

(see Ref. 10 for a one-dimensional problem). The heating rate is  $n\omega$ ; therefore if we define some arbitrarily small region about the heat source, the percentage of total heat restricted to that region will be greater at the higher frequencies. However, the phase of the temperature at a point away from the source, relative to the maximum temperature at the source (on the upper surface of the cantilever), is almost a linearly increasing function of distance (Fig. 3). Thus, before a distant point attains its maximum possible temperature (compatible with a given power input), the source is already so much lower in temperature that it effectively competes as a sink for the outward heat flux. This implies that the temperature is a maximum at the lowest frequency (Figs. 4 and 5; ac power is about 1 mW).

The cantilever is bent by preferential heating on the upper surface, according to the forcing function

$$\partial_x^2 \int_{-h/2}^{h/2} y T(x, y, t) dy.$$

If the temperature is constant in either the x or the y direction, or is a linear function of x, then the forcing function and strain are zero.

At very low frequencies of heat input, the temperature is fairly constant along x and y; hence it contributes neglibly to the strain. The largest drop in temperature along y, for  $0 \le x \le L$ , occurs at the pedestal edge, because this is also the first point of the heat sink. This point is further complicated because

$$w(0^-, t) = 0$$

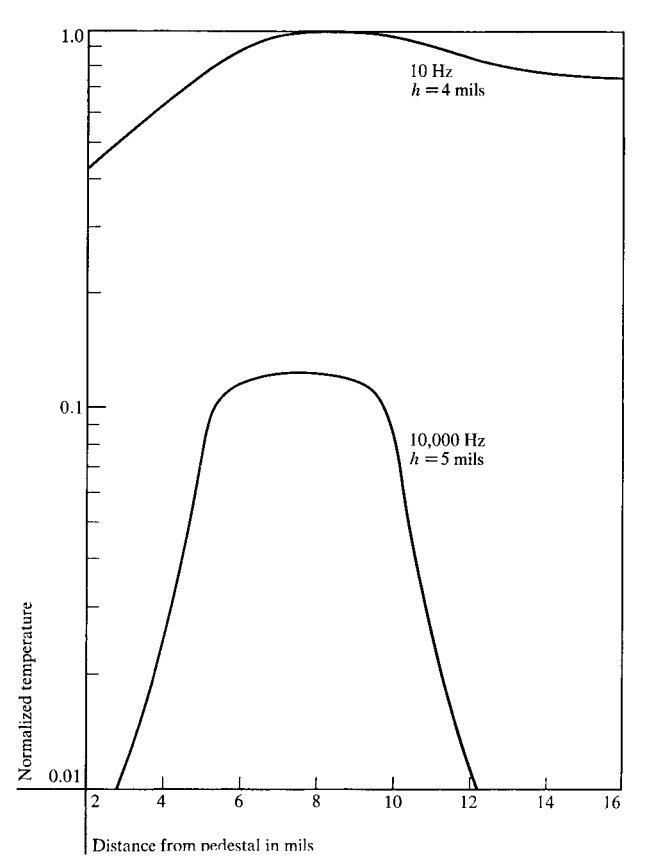


Figure 5 Normalized temperature  $|\varphi(x)|/|\varphi_{\text{source}}, \omega = 10 \text{ Hz}|$  at the upper surface vs. distance from the pedestal edge (x=0).

and all its higher derivatives are zero, whereas w is certainly not zero at  $x = 0^+$ . Generally the strain at x = 0 (the pedestal edge) is a maximum. From the above equation we can intuitively postulate that to minimize the radius of curvature

$$\left[\partial_x^2 T(x, y, t)\right]^{-1}$$

of the temperature distribution in the x direction (and hence maximize its inverse), the heating element must be sufficiently isolated from the sink that the temperature can build up to a sharp peak, yet not so isolated that decay in the x direction is too slow. There is a compromise in maximizing the temperature drop along y to obtain maximum strain. Figure 6 indicates that, to optimize strain for a device of the specified geometry, the heater element must be located within a certain range of the pedestal: 3 mils  $\leq x = a \leq 16$  mils. For heaters whose inside edges are located at x = 0 and x = -2 mils, respectively, the strains measured at the pedestal are lower, by 17\% and 49\% respectively, than the lowest value measured for a heater within the optimum range. As shown by Fig. 6, for heaters within the optimum range of x the strain varies from maximum to minimum by only 2.9%.

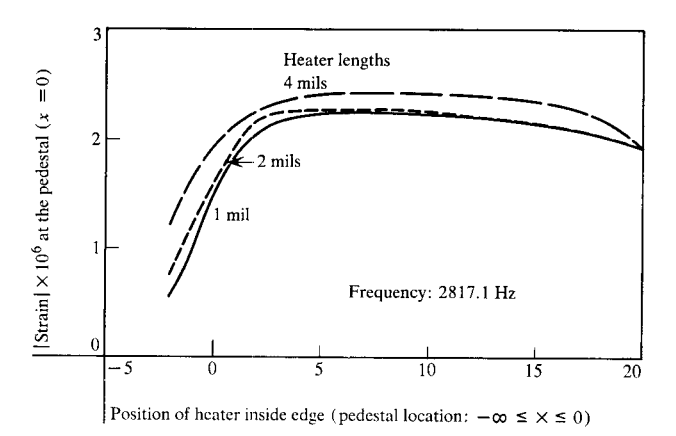
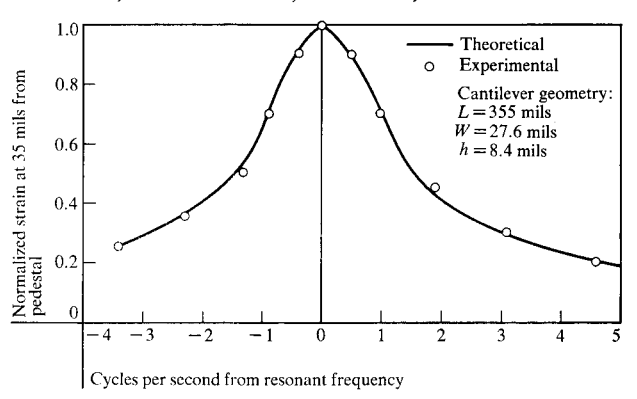


Figure 6 Maximum strain at the upper surface vs. distance from the pedestal edge (x = 0).

Figure 7 Maximum strain at x = 35 mils vs. driving frequency. (Experimental strain normalized to 3.62, theoretical strain to 1.13; both  $\times 10^{-6}$ . Experimental resonant frequency, 3645.5 Hz; theoretical value, 3609.1 Hz.)



As is true for most mechanical vibrating devices, the cantilever is very sensitive to driving frequency. This dependency is shown in Fig. 7, where relative peak strain at a point 35 mils from the heat sink is plotted against driving frequency. The calculated Q of 1900 is in excellent agreement with the experimental value of 1950. The empirical damping coefficient c is based on a Q of 1950, and its consistency is confirmed by this agreement.

The experimental values of strain were measured with a piezoresistive bridge fabricated as part of the cantilever. Again, the very good agreement between the analytical and experimental curves confirms the mathematical model.

The strain distribution is linearly dependent on  $V_B$  and  $V_G$  but, from the discussion of temperature, we observe that maximizing  $V_B$  minimizes the power channeled into the  $2\omega$  mode. If  $\omega$  is the resonant frequency, this maximization best utilizes the input power.

Resonant frequency is plotted against strain for several cantilever lengths in Fig. 8. The curve indicates that there is an optimal resonant frequency or length. (The experimental points were obtained by sand-trimming the cantilever length, a process which changes the value of Q. Each experimental point therefore lies on a separate curve, corresponding to the different values of Q. The theoretical curve, however, was computed only for Q = 1950.)

#### Summary

A simplified model for a transverse vibrating beam has been shown to characterize the cantilever very well. The forcing function is dependent on temperature field, which is found by the method of images. Time-dependent contributions to the temperature distribution are conveniently included in the well-tabulated modified Bessel function  $K_0$ .

If Green's functions are used to solve the equation of motion, the solution can be given in integral form. This is advantageous if the temperature forcing function is in discrete form, especially since its derivatives are needed.

Variation of input parameters has led to optimum design for the cantilever, as can be inferred from the graphs and the discussion of results. Computer runs that simulate additional experimental devices give strains which are of the correct order of magnitude. Both the experiments and the simulation foster confidence in the model as to its characterization of device behavior for design purposes.

# **Acknowledgments**

The authors thank J. W. Cooley, T. D. Schultz, R. J. Wilfinger and Z. C. Putney for helpful discussions. Thanks are due also to F. D. Jones for experimental support.

## References

- R. J. Wilfinger, P. H. Bardell and D. S. Chhabra, "The Resonistor—A Frequency Selective Device Utilizing the Mechanical Resonance of a Silicon Substrate," *IBM J. Res. Develop.* 12, 113 (1968).
- H. Goldstein, Classical Mechanics, Addison-Wesley Press, Inc., Cambridge, Mass., 1951, pp. 275–284.
- L. Landau and E. Lifshitz, Theory of Elasticity, Second Ed., Addison-Wesley Publishers, New York, 1964, pp. 6-20.

Experimental values 0		
Length (mils)	Resonant Frequency (kHz)	Q
355	3.6455	1950
317	4.5135	1560
282	5.6443	1680
227	8.2964	1170
186	12.028	1410
146	19.405	~500

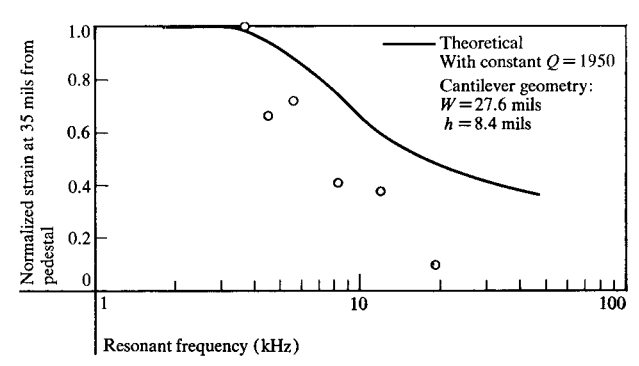


Figure 8 Maximum strain at x = 35 mils vs. driving frequency as a function of cantilever length. (Strain normalized to lowest frequency, as in Fig. 7.)

- B. A. Boley, "Thermally Induced Vibration of Beams," J. Aero Sciences 23, 179 (1956).
- B. A. Boley, Theory of Thermal Stresses, John Wiley and Sons, New York, 1960.
- H. S. Carslaw and J. C. Jaeger, Conduction of Heat in Solids, Second Ed., Oxford University Press, London, 1959, pp. 173-181.
- A. Ralston, First Course in Numerical Analysis, First Edition, McGraw-Hill Publishing Co., Inc., New York, 1965, p. 400.
- M. Abramowitz and I. A. Stegun, Handbook of Mathematical Functions, Fourth Ed., National Bureau of Standards, 1944, pp. 379-385.
- A. G. Webster, Partial Differential Equations of Mathematical Physics, Dover Publications, New York, 1955.
- H. S. Carslaw and J. C. Jaeger, Conduction of Heat in Solids, Second Ed., Oxford University Press, London, 1959, p. 66.

Received July 1, 1968 Revised April 1, 1969